JOURNAL OF SOLID STATE CHEMISTRY 119, 254–259 (1995)

Preparation and Structure of $BiCaRu_2O_{7-y}$

Brendan J. Kennedy

The School of Chemistry, The University of Sydney, New South Wales 2006, Australia

Received December 19, 1994; accepted May 9, 1995

The structure of $(BiCa)Ru_2O_{7-y}$, space group $Fd3m$, a = 10.2246(1) Å, y = 0.14, has been determined by Rietveld analysis of room temperature powder neutron diffraction data. The XPS of the compound displays two Ru 3*d* doublets due to screening effects. The magnetic properties of the material between 4 and 300 K are reported. © 1995 Academic Press, Inc.

INTRODUCTION

Ternary ruthenium oxides adopting the cubic pyrochlore structure, of the general form $A_2B_2O_6O'$, are of considerable interest for use as electrode materials, as thin film resistors, and as oxidation catalysts (1–8). It appears that both the electronic properties of these materials and their reactivity are related to the extent of oxygen nonstoichiometry and/or to the precise Ru–O–Ru contacts (9, 10). As part of a wider study of the relationship between the electronic properties, the presence and site occupancies of oxygen nonstoichiometry, and the electrochemical properties of pyrochlore oxides (11–14), the mixed metal pyrochlore $(BiCa)Ru_2O_{7-y}$ has been prepared and characterized.

EXPERIMENTAL

Analytical grade Bi_2O_3 and $CaCO_3$ were dried at 900°C and 300°C, respectively, before use. Stoichiometric amounts of Bi_2O_3, $CaCO_3$, and Ru (1 : 2 : 4) were intimately mixed in an agate mortar and pestle. The mixture was fired in an alumina crucible at 650°C for 1 hr to drive off CO_2, followed by 3 × 1 day + 4 days at 800°C, 2 days at 900°C, and 2 × 2 days at 1000°C with intermediate grindings between each heating step (15). All heating was done in air. Powder X-ray diffraction measurements, recorded on a Siemens D-5000 diffractometer, confirmed the presence of a single-phase pyrochlore-type material.

X-ray photoelectron spectra were collected using a Kratos XSAM 800 spectrometer with Mg$K\alpha$ (1254.6 eV) radiation at 15 kV, 10 mA. A pass energy of 80 eV was used to collect a survey scan, and individual regions were collected with a pass energy of 20 eV. No unexpected peaks were observed in the survey scan. All binding energies were referenced to the C 1*s* signal at 284.6 eV. The operating pressure was below 10^{-9} Torr. Scanning electron micrograph images were collected with a Philips SEM 505. Magnetic susceptibility data were collected at 0.5 and 1 T between 4 and 300 K using a SQUID device.

Powder neutron diffraction data were collected over the range $0 < 2\theta < 155°$ in 0.05° steps on the HRPD at ANSTO's HIFAR reactor using neutrons of wavelength 1.4925 Å (16). The final profile was obtained from a weighted average of the eight counters on the HRPD. The lightly ground sample was contained in a thin-walled 12-mm-diameter vanadium can which was rotated during the measurements to reduce the effects of preferred orientation.

The structure refinement was undertaken with the PC version of the computer program LHPM (17), which uses a full profile Rietveld analysis (18). The background was defined by a fourth-order polynomial in 2θ and was refined simultaneously with the other profile and structural parameters. A Voigt peak shape function was employed, where the Gaussian component has widths given by the Caglioti, Paoletti, and Ricci function (19),

$$\mathrm{FWHM}^2 = U \tan^2\theta + V \tan\theta + W,$$

with refinable parameters U, V, and W. The widths of the Lorentzian component varied as $\eta \sec\theta$ to model particle size effects and a peak asymmetry parameter was included. The coherent scattering lengths used were Ru, 0.7210; Bi, 0.8533; Ca, 0.4900; and O, 0.5805 × 10^{-12} cm (20). The refinement was considered to have converged when all the parameter shifts were less than 10% of their associated e.s.d's in the last cycle. Final parameters are given in Table 1. The final R factors were R_p = 6.89, R_{wp} = 8.80, R_{exp} = 4.47, and R_B = 1.17%.

RESULTS AND DISCUSSION

Scanning electron micrographs of the material showed it to be highly crystalline with particles of about 400 nm diameter. The individual crystallites are well formed, al-

0022-4596/95 $12.00

TABLE 1
Atomic Coordinates and Thermal Parameters (10^{-3} Å^2) for $BiCaRu_2O_7$ at Room Temperature

Atom	Site	x	y	z	Occupancy	U_{11}	$U_{22} = U_{33}$	$U_{12} = U_{13}$	U_{23}
Bi/Ca	16*d*	0.5	0.5	0.5	1.0	13.3(5)	U_{11}	−2.9(4)	U_{12}
Ru	16*c*	0	0	0	0.97(1)	2.7(5)	U_{11}	−0.6(4)	U_{12}
O	48*f*	0.3256(1)	0.125	0.125	1.0	9.5(5)	7.3(4)	0	2.5(5)
O′	8*b*	0.375	0.375	0.375	0.86(2)	15.4(1.6)	U_{11}	0	0

though obviously intergrown (see Fig. 1), and there is no evidence either for segregation of Ca from the material or for an amorphous phase.

Refinement of the powder neutron diffraction profiles proved straightforward. Examination of the profiles gave no evidence for any lowering of the symmetry such as occurs in, for example, $Pb_2Ru_2O_{6.5}$, where there is an ordering of the oxygen site vacancies (7), and so refinement was undertaken in space group *Fd*3*m*. Refinements in which the occupancies of both Bi and Ca were varied, both simultaneous and independently, gave values within 1 e.s.d. of the expected value, and these sites were constrained to be fully occupied in the final cycles. The occupancies of both the Ru and the O(2) sites were found to be significantly less than the stoichiometric values and indicate a final stoichiometry of $(BiCa)Ru_{1.97}O_{6.86}$. The slight ruthenium deficiency is presumably due to the formation of the volatile RuO_4 species during the preparation. Figure 2 shows the observed and calculated neutron diffraction profiles of $BiCaRu_2O_{7-y}$. The final crystallographic parameters are listed in Table 1.

Mg*K*α X-ray photoelectron spectra of the Ru 3*d* and Bi 4*f* core levels of $(BiCa)Ru_2O_{7-y}$ are shown in Fig. 3. The Ru 3*d* doublet overlaps with the C 1*s* line, and it is

FIG. 1. Scanning electron micrographs of $(BiCa)Ru_2O_{7-y}$.

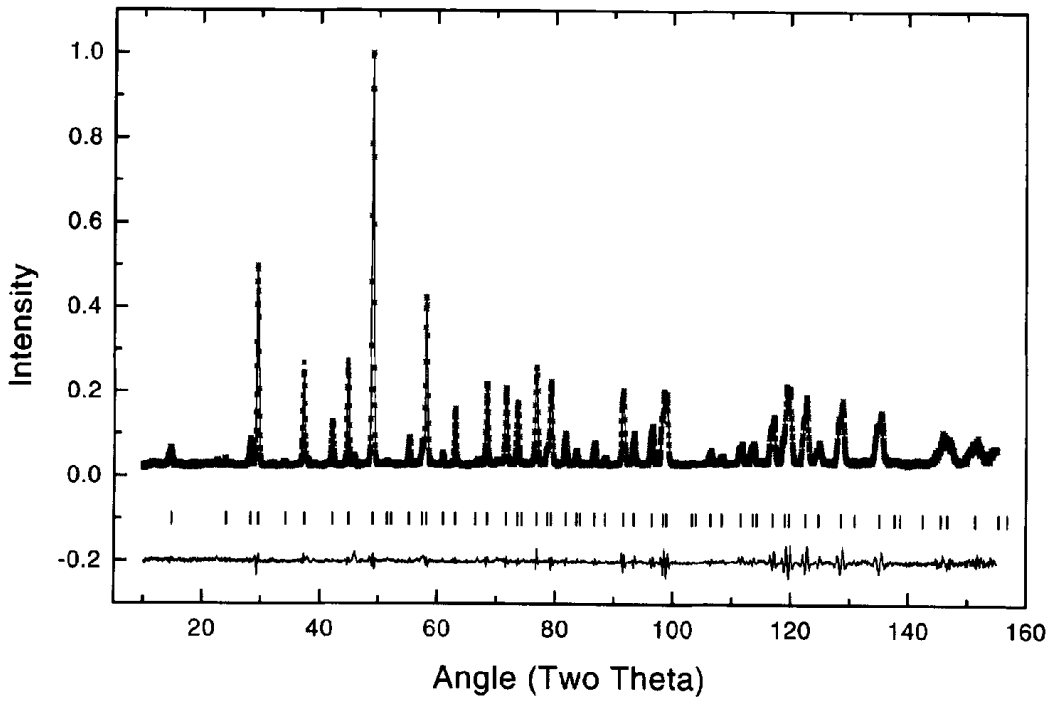

FIG. 2. Observed, calculated, and difference neutron powder diffraction profiles for $BiCaRu_2O_{7-y}$. The observed data are indicated by crosses and the calculated profile by the solid line. The short vertical lines below the profiles mark the position of all possible Bragg reflections.

necessary to utilize a number of constraints in the analysis of the spectra. The protocol used was to fit the intensity near 281 eV to a single Ru $3d_{5/2}$ line and then to construct the corresponding Ru $3d_{3/2}$ line using standard constraints (14, 21). A C 1*s* line was then added near 284.6 eV and then the unfitted intensity near 282.5 eV was fitted to a second Ru 3*d* doublet. Finally the region above 285 eV was fitted with an additional C 1*s* line, giving a measure of fit of 2.61%. As evident from Fig. 2, two Ru 3*d* doublets, of approximately equal intensity, are observed, and it is tempting to ascribe these to Ru(IV) and Ru(V) species. While it is difficult to interpolate between the neutron diffraction and XPS results, the presence of two Ru 3*d* doublets, with the higher BE having lower intensity, suggesting that there is a slight deficiency of Ru(V), is consistent with the need to charge balance for the oxygen deficiency. Such an explanation, while pleasing in its simplicity, is inconsistent with the pyrochlore structure in which a single Ru site is present. A more likely explanation of the XPS results is that the doublet at lower BE is due to screening of the Ru 4*d* levels by the conduction electrons (6, 22). If this is true then the XPS of all atoms involved in the conduction should also exhibit the effects of screening. The Bi 4*f* doublets are noticeably asymmetric toward higher BE, as is the O 1*s* peak. This has been observed in both the metallic oxides $Bi_2Ru_2O_{6.9}$ and the nonpyrochlore material $Bi_3Ru_3O_{11}$ and is ascribed to the combined effects of both slight surface segregation of a Bi species and screening by the conduction electrons. The Ca 2*p* line is a simple doublet. The photoelectron spectrum of the Ru 4*d* conduction band region is similar to that found for $CaRuO_3$ (5) in that it shows a poorly resolved conduction band shape with a small Fermi edge suggesting that electron–electron interactions are important.

The magnetic properties of the material between 4 and 300 K have been determined and are shown in Fig. 4. It is apparent that the material does not exhibit the weak Pauli temperature-independent paramagnetism typical of metals, but rather shows Curie–Weiss type behavior with the magnetic moment decreasing from 1.99 BM at 300 K to 0.3 BM at 4.2 K. This behavior cannot be readily explained in terms of coupling of the spins of localized Ru (IV) and Ru (V) centers, but rather suggests delocalization of the spin of the system. The Ru (IV) perovskites $CaRuO_3$ and $SrRuO_3$ are metallic, but both have large temperature-dependent susceptibilities, presumably as a consequence of enhancement of exchange interaction between electrons in the conduction band, a Stoner enhancement (22). Preliminary conductivity measurements show the present material to exhibit high conductivity, which together with the poorly resolved Fermi edge observed in the photoelectron spectra suggest the material is metallic. Unfortunately it has not been possible to prepare single crystals to confirm this. Cox and co-workers have shown that the Ru 4*d* conduction band in ruthenium pyrochlores

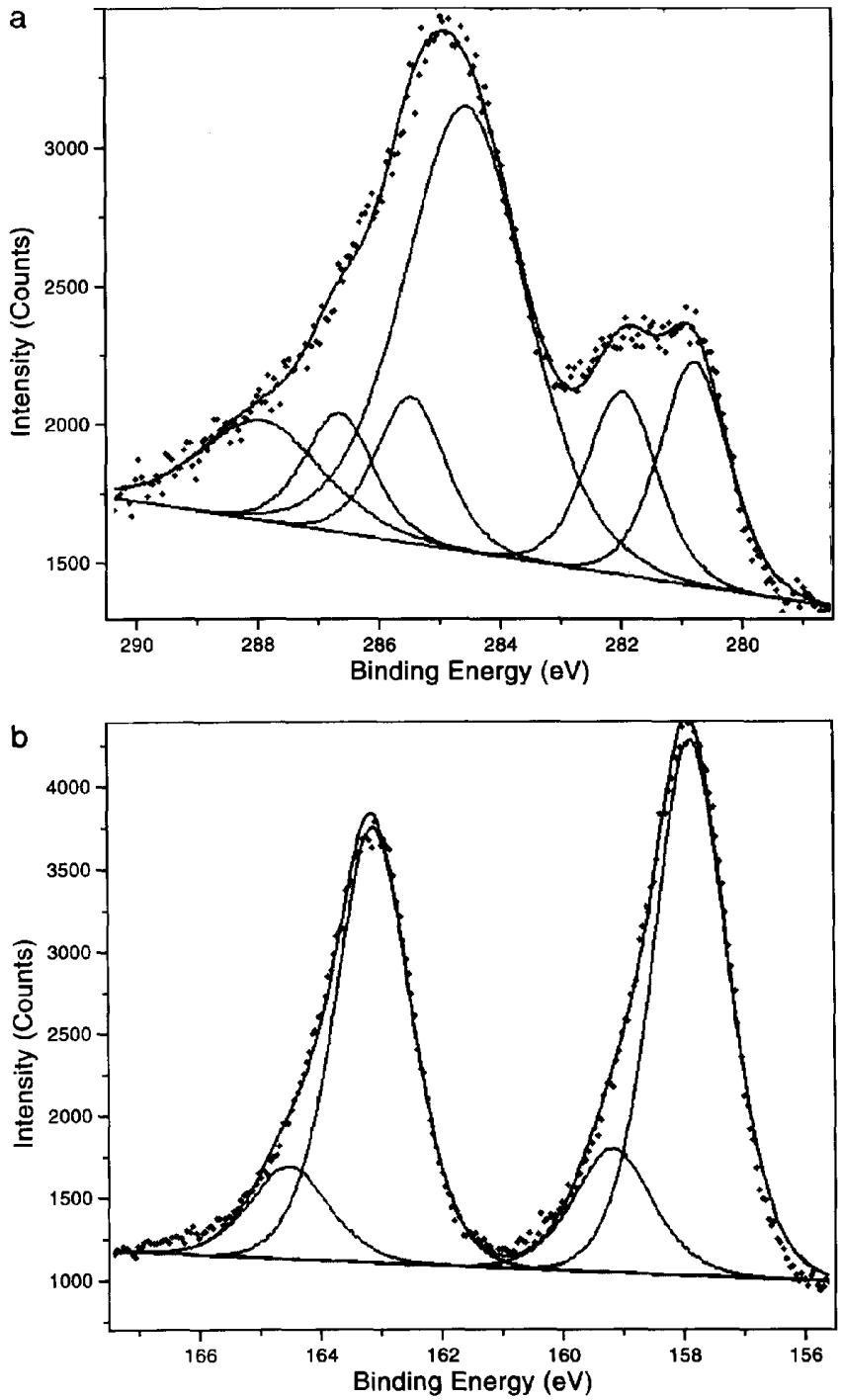

FIG. 3. X-ray photoelectron spectra of (a) the Ru 3*d* and C 1*s*, and (b) the Bi 4*f* regions of $(BiCa)Ru_2O_{7-y}$.

is relatively narrow (22, 23), which enhances electron–electron interactions and consequently the paramagnetism of the complex. The weight of evidence suggests that a similarly narrow conduction band is present in (BiCa) Ru_2O_{7-y}.

High resolution neutron diffraction data for a number of ruthenium-containing pyrochlores are now available and are summarized in Table 2. The unit cell length in $(BiCa)Ru_{1.97}O_{6.86}$, 10.2246(7) Å, is slightly (≈ 0.7%) smaller than found in $Bi_2Ru_2O_{6.9}$ (14), 10.2957(1) Å, in keeping with the smaller ionic radius of Ca^{2+} vs Bi^{3+} as well as with the formal decrease in the Ru oxidation state

TABLE 2
Structural Parameters for a Number of Ruthenium Pyrochlores of the Type A_2Ru2O_{7-y}

A	Bi_2	BiCa	PbBi[a]	Pb_2[a]	Tl_2(HT)	Tl_2(LT)	Y_2
a (Å)	10.2957	10.2246	10.2519	10.2758	10.2008	10.2116	10.1429
y	0.08	0.14	0.50	0.50	0.29	0.00	0.00
Ru–O (Å)	1.984	1.966	1.987	1.969	1.953	1.970	1.991
			1.963	1.954			
A–O(6) (Å)	2.550	2.539	2.573	2.563	2.549	2.523	2.450
			2.533	2.564			
A–O(2) (Å)	2.229	2.214	2.211	2.260	2.209	2.211	2.196
Ru–O–Ru (°)	133.14	133.69	134.95	134.81	134.88	132.74	128.45
Ref.	(14)	This work	[b]	(7)	(9)	(9)	(8)

[a] Ordering of the oxygen vacancies occurs, see reference (7).
[b] B. J. Kennedy and M. M. Elcombe, unpublished observations.

from 4.5 to 4. This contraction in unit cell length is reflected by a 0.9% decrease in the Ru–O bond lengths to 1.966(1) Å, compared to 1.984(1) Å in $Bi_2Ru_2O_{6.9}$. The Bi(Ca) oxygen distances, two at 2.214(1) and six at 2.539(1) Å, are also about 0.6% smaller than observed for $Bi_2Ru_2O_{6.9}$, 2.229 and 2.550 Å, respectively.

It is informative to note that while the Ru–O–Ru angle in metallically conducting Ru pyrochlores is larger than that found in semiconducting samples such as $Y_2Ru_2O_7$ (8) or $Tl_2Ru_2O_7$ (9) prepared at high temperatures, this difference is relatively small and can, in part, be explained by changes in the size of the unit cell. In pyrochlore oxides, as the unit cell dimension increases, so too does the B–O–B angle. A more striking observation is the persistence of oxygen vacancies in the metallic pyrochlores such as $Pb_2Ru_2O_{6.5}$ or $Bi_2Ru_2O_{6.9}$. There is appreciable oxygen nonstoichiometry in $(BiCa)Ru_2O_{6.86}$, suggesting this is in fact also a metallic oxide. Further studies exploring this observation are in progress and will be reported in due course.

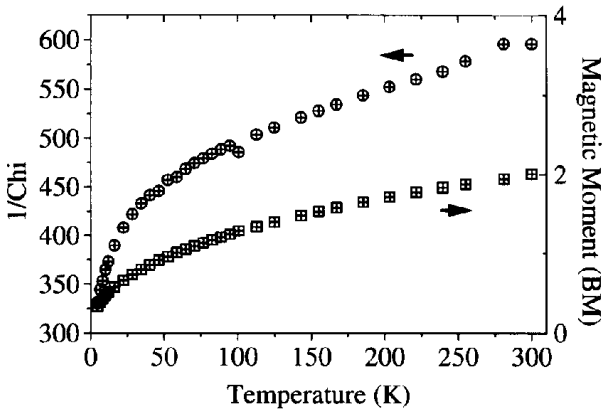

FIG. 4. Magnetic moments (⊞) and reciprocal susceptibility (⊕) (per Ru) vs temperature for $BiCaRu_2O_{7-y}$.

ACKNOWLEDGMENTS

This work has been supported by the Australian Research Council and the Australian Institute of Nuclear Science and Engineering. The magnetic susceptibility data were kindly collected by Drs. K. S. Murray and B. Moubaraki at Monash University, and the assistance of Dr. D. Argriou in recording the neutron diffraction data is gratefully acknowledged.

REFERENCES

1. H. S. Horowitz, J. M. Longo, and J. T. Lewandowski, *Mater. Res. Bull.* **16,** 486 (1981).
2. H. S. Horowitz, J. M. Longo, and H. H. Horowitz, *J. Electrochem. Soc.* **130,** 1851 (1983).
3. R. Manoharan and J. B. Goodenough, *J. Electrochem. Soc.* **137,** 910 (1990).
4. A. T. Ashcroft, A. K. Cheetham, J. S. Foord, M. L. H. Green, C. P. Grey, A. J. Murrell, and P. D. F. Vernon, *Nature* **344,** 319 (1990).
5. R. G. Edgell, J. B. Goodenough, A. Hamnett, and C. C. Naish, *J. Chem. Soc. Faraday Trans. 1* **26,** 155 (1983).
6. P. A. Cox, J. B. Goodenough, P. J. Tavener, D. Telles, and R. G. Edgell, *J. Solid State Chem.* **62,** 360 (1986).
7. R. A. Beyerlein, H. S. Horowitz, J. M. Longo, M. E. Leonowicz, J. D. Jorgensen, and F. J. Rotella, *J. Solid State Chem.* **51,** 253 (1984).
8. B. J. Kennedy, *Acta Crystallogr. Sect. C* **51,** 750 (1995).
9. R. Kanno, J. Huang, and A. W. Sleight, *in* "Proceedings of the 5th International Symposium on Advance Nuclear Energy Research," p. 347. (1993).
10. R. Kanno, Y. Takeda, T. Yamamoto, Y. Kawamoto, and O. Yamamoto, *J. Solid State Chem.* **102,** 106 (1993).
11. G. Gokagac and B. J. Kennedy, *Langmuir* **9,** 1862 (1993).
12. G. Gokagac and B. J. Kennedy, *J. Electroanal. Chem.* **353,** 71 (1993).
13. G. Gokagac and B. J. Kennedy, *J. Electroanal. Chem.* **368,** 235 (1994).
14. G. R. Facer, M. M. Elcombe, and B. J. Kennedy, *Aust. J. Chem.* **46,** 1897 (1993).
15. E. Beck and S. Kemmler-Sack, *Mater. Res. Bull.* **21,** 307 (1986).
16. C. J. Howard, C. J. Ball, R. L. Davis, and M. M. Elcombe, *Aust. J. Phys.* **36,** 507 (1983).

17. R. J. Hill and C. J. Howard, "Australian Atomic Commission Report No. M112, AAEC (now ANSTO)," Lucas Heights Research Laboratories, New South Wales, Australia, 1986.
18. H. M. Rietveld, *J. Appl. Crystallogr.* **2,** 65 (1969).
19. G. Caglioti, A. Paoletti, and F. P. Ricci, *Nucl. Instrum.* **3,** 223 (1958).
20. V. F. Sears, "Atomic Energy of Canada Report No. AECL-8490." 1984.
21. T. R. Felthouse, P. B. Fraudorf, R. M. Friedman, and C. Schosser, *J. Catal.* **157,** 421 (1991).
22. P. A. Cox, "Transition Metal Oxides—An Introduction to their Electronic Structure and Properties." Clarendon, Oxford, 1992.
23. P. A. Cox, R. G. Edgell, J. B. Goodenough, A. Hamnett, and C. C. Naish, *J. Phys. C Solid State Phys.* **16,** 6221 (1983).